

CYCLIC PERFORMANCE OF HOT-DRIVEN RIVETED CONNECTIONS

Aldo Milone¹

¹ Department of Structures for Engineering and Architecture
Via Forno Vecchio 36, 80134, Naples, Italy
e-mail: aldo.milone@unina.it

Abstract

Riveted connections represent one of the most common structural details adopted in existing steel bridges. Due to the increase of traffic loads as respect to the conditions at their erection time, existing riveted bridges are usually characterized by structural deficiencies and prone to fatigue damages. Nevertheless, in current normative provisions (EN1993:1-9) no indications are given about assessing the fatigue performance of such connections. In this paper, results from experimental cyclic tests on riveted lap shear connections are presented and discussed. The considered connections are representative of typical details found in actual existing railway bridges. The influence of connection geometry on the fatigue performance is investigated by varying the following parameters, namely: (i) connection configuration, (ii) number of rivets, (iii) diameter of rivet shank, (iv) plates thickness.

Keywords: Fatigue, Riveted Connections, Steel Bridges, Hot-Driving

1 INTRODUCTION

Hot-driven riveted connections represent one of the most common type of structural details adopted in railway bridges located Italy (≈ 3500) [1]. This kind of structural typology had its heyday among the XIXth century and the first half of the XXth century, before being gradually replaced by high-strength bolted connections [2]. Hence, existing Italian riveted railway bridges have often already endured an exceptionally long service life. This inevitably exposes such kind of structures to critical fatigue issues [1,2].

Nevertheless, European fatigue design provisions in force referred to steel structures (EN1993:1-9 [3]) do not provide any indication about fatigue assessment of hot-driven riveted connections. For instance, a lone detail class $\Delta\sigma_C = 71 \text{ N/mm}^2$ was suggested by EN1993:1-9 background document, thus completely disregarding the widely recognized influence of actual joint detailing on the structural behaviour [4-25]. Such detail class has been subsequently removed in the final draft of EN1993:1-9.

Therefore, in the present paper the fatigue performance of multiple configurations of lap-shear hot-driven riveted connections is parametrically investigated by means of numerical analyses. Namely, an application of the SED method [26-28] is carried out *i)* with reference to a preliminary set of fatigue tests and *ii)* to investigate the influence of connections geometry on the fatigue performance. To this end, refined finite element models (FEMs) are developed.

The present work is divided in three parts. In the first section, the main features of investigated riveted connections are presented; the most relevant modeling assumptions are re-reported in the second part, with particular attention to FEM-based SED calculations. Finally, the results of numerical analyses are discussed, highlighting the influence of the investigated parameters on cyclic response of considered riveted joints.

2 GEOMETRICAL FEATURES OF INVESTIGATED CONNECTIONS

In the present work, eleven different types of lap shear riveted connections are tested in order to evaluate the influence of *(i)* rivet diameter, *(ii)* plates width and thickness and *(iii)* number of rivets on both static and fatigue behavior of these joints. Each adopted configuration is representative of typical details adopted in existing railway bridges (Figure 1) [1,2].

A proper nomenclature *C-D-T-N-R* is hence introduced to label each investigated joint, where:

L refers to the joint configuration, i.e., symmetric or unsymmetric;

D refers to the rivet diameter (16, 19 or 22 mm);

T refers to the plate thickness (10 or 12 mm);

N refers to the number of rivets (1 or 2);

R refers to the control volume radius R_0 ($0.1 \div 1.5 \text{ mm}$), i.e., a material parameter governing fatigue life estimations according to the SED method [26-28].

A total of $29 \times 11 = 319$ finite element analyses (FEAs) were carried out accounting for the variation of each introduced parameter (see Table 1).

Table 1: Main geometrical features of investigated joints.

Label	Configuration	Rivet Diameter	Plate Thickness	Number of Rivets	Control Volume Radius
[-]	[-]	D [mm]	T [mm]	N	R [mm]
S-16-10-1-R	Symmetric	16	10	1	0.10 ÷ 1.50 (Increments of 0.05 mm)
S-19-10-1-R	Symmetric	19	10	1	
S-19-10-2-R	Symmetric	19	10	2	
S-22-12-2-R	Symmetric	22	12	2	

U-19-10-2-R	Unsymmetric	19	10	2	0.10 ÷ 1.50 (Increments of 0.05 mm)
U-22-12-2-R	Unsymmetric	22	12	2	
S-19-12-1-R	Symmetric	19	12	1	
S-22-10-1-R	Symmetric	22	10	1	
S-22-12-1-R	Symmetric	22	12	1	
U-19-10-1-R	Unsymmetric	19	10	1	
U-19-12-1-R	Unsymmetric	19	12	1	

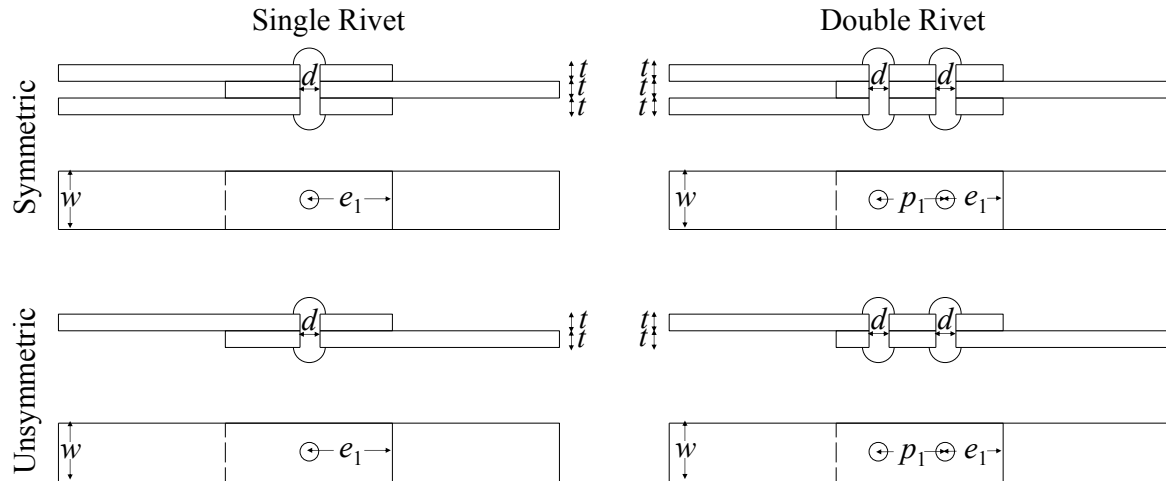
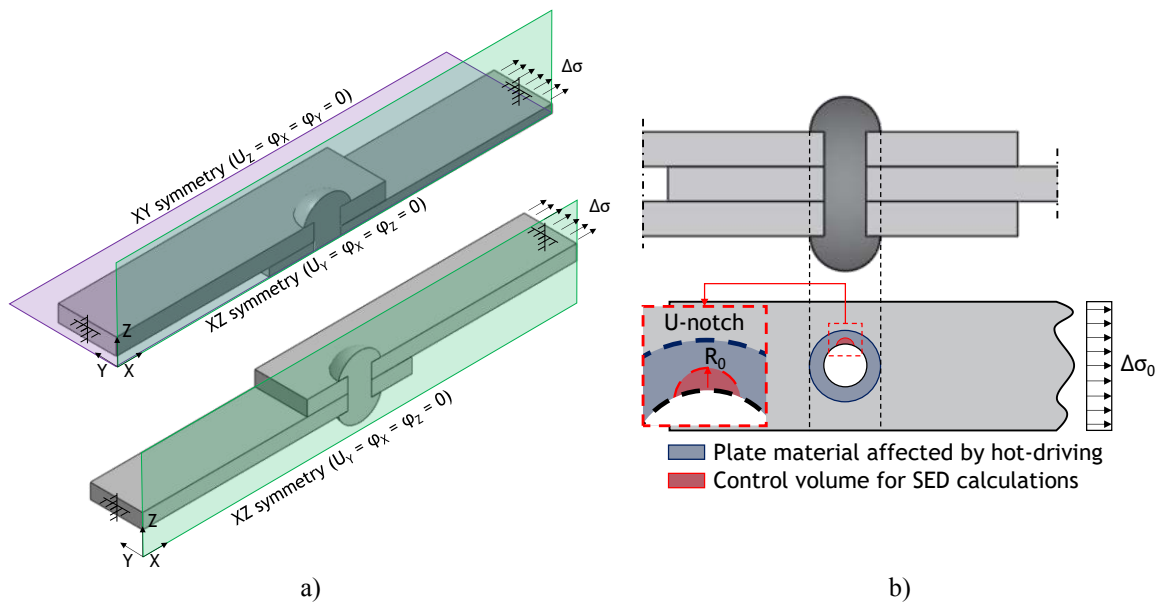


Figure 1: Main geometrical features of investigated joints.

3 MODELLING ASSUMPTIONS

Finite element models (FEMs) were developed using ABAQUS 6.14 [29]. With the aim to balance analyses accuracy and computational effort, riveted connections were modelled explicitly accounting for their geometrical and mechanical symmetry. Fatigue behavior of each connection has been investigated imposing stress ranges on the free end of connected plates. Adopted boundary conditions (BCs) are reported in Figure 2a.



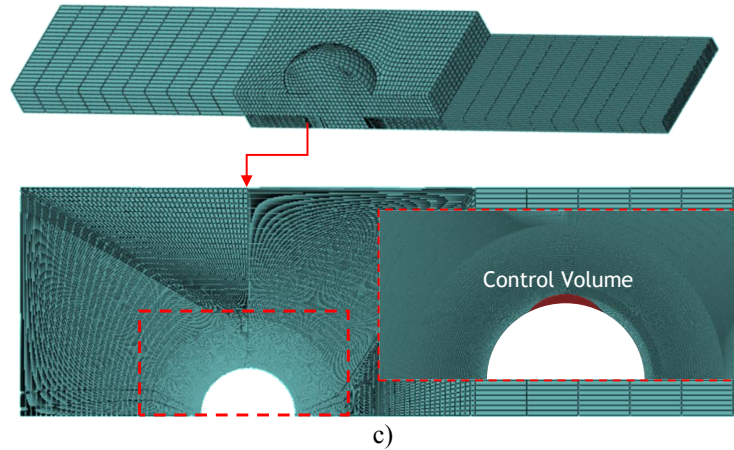


Figure 2: a) BCs and b) adopted mesh for FEAs and c) definition of the control volume for SED calculations.

All elements were discretized using solid C3D8 element type (i.e. 8-node linear brick). The mesh density was defined on the basis of indications reported in [27-28]; therefore, a minimum mesh size $s = 0.05$ mm was set nearby the rivet hole, a value of 1 mm was adopted for the rest of the connection zone, while a coarse mesh having $s = 20$ mm was adopted for the plates ends, which were not expected to endure fatigue damage (Figure 2c). An “Hard Contact” formulation was considered for the normal contact behavior, while a penalty formulation was used to model the tangential behavior (with friction coefficient $\mu = 0.30$).

According to SED method basic assumptions [26-28], fatigue performance of connections has been monitored through the averaged strain energy density (ASED) range ΔW [mJ/mm³] measured in a moon-shaped, R_0 -wide control volume centered at the hole quadrant (Figure 2b).

4 RESULTS

4.1 Interpretation of experimental fatigue tests

A first application of the SED method to assess the fatigue performance of hot-driven riveted connections was first carried out with respect to experimental fatigue tests performed within the framework of ReLuis – CSLLP 2022-2024 Italian research project.

Up to present time, six zero-to-tension fatigue tests ($R = \sigma_{\min}/\sigma_{\max} = 0$) have been performed on both unsymmetric and symmetric specimens complying with geometrical features reported in Table 1. Interpretation of results via SED method are summarized in Figure 3 and Table 2.

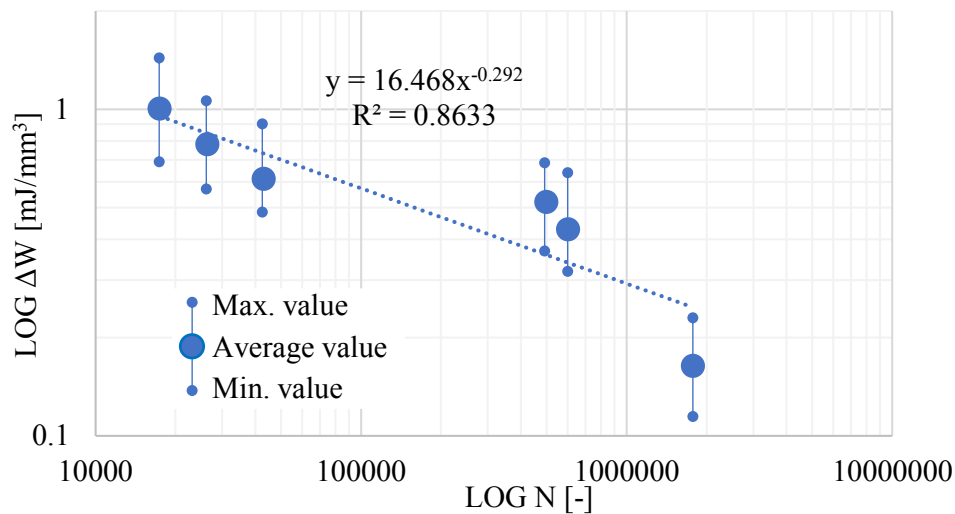


Figure 3: Interpretation of experimental results through the SED method.

Table 3: Interpretation of experimental results through the SED method.

Label	Applied Load Range	ASED Range	Cycles at Failure
[-]	ΔF [kN]	ΔW [mJ/mm ³]	N [-]
S-22-12-2-R	160	0.57	$4.9 \cdot 10^5$
U-22-12-2-R	160	1.08	$1.7 \cdot 10^4$
U-22-12-2-R	145	0.84	$2.6 \cdot 10^4$
U-19-10-2-R	100	0.63	$4.2 \cdot 10^4$
S-19-12-1-R	115	0.48	$6.0 \cdot 10^5$
S-22-12-1-R	50	0.17	$1.7 \cdot 10^6$

Reliability of SED method in assessing the fatigue performance of hot-driven riveted specimens is proved by the rather high coefficient of determination $R^2 = 0.86$.

4.2 Parametrical analyses

After proving the reliability of SED method, parametrical analyses on hot-driven riveted connections have been performed to investigate the influence of geometrical features on the fatigue performance of assemblies. Hence, all considered specimens reported in Table 1 have been assessed considering a nominal stress range $\Delta\sigma = 71 \text{ N/mm}^2$, i.e., coincident with the detail class reported in the EN1993:1-9 background document.

According to [26-28], ASED range for a holed plate (U-notch) can be expressed according to Equation 1:

$$\Delta W = \frac{(k \Delta\sigma)^2}{2E} \quad (1)$$

where k is an equivalent stress magnification factor (SMF) expressing the influence of geometry on the fatigue performance of specimens and E is the material Young Modulus (210000 N/mm^2).

Hence, as FEM-based ASED calculations were performed, k could be derived according to the above expression. Results in terms of k for each considered geometry are summarized in Figure 4.

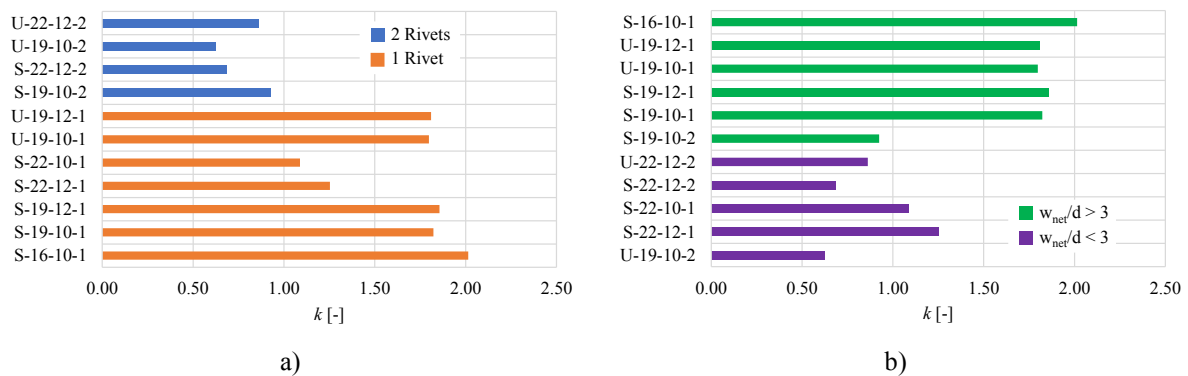


Figure 4: Influence of geometrical features on the fatigue performance: a) number of rivets N, b) bearing ratio w_{net}/d .

It can be noticed that the most influent parameters on fatigue performance of riveted connections are *i*) the number of rivets N, with enhanced performance for multiple rivets specimens and *ii*) the so-called bearing ratio w_{net}/d , with w_{net} being the net width of the plate in correspondence of the rivet hole. These results comply with outcomes reported in [30].

5 CONCLUSIONS

In the present work, the fatigue performance of hot-driven riveted connections was parametrically investigated through a FEM-based application of the SED method. Based on achieved results, the following conclusions can be pointed out:

- The effectiveness of SED method in assessing fatigue performance of riveted assemblies has been proved with respect to experimental tests on actual hot-driven specimens;
- The influence of geometrical features on the fatigue performance of hot-driven specimens has been preliminary assessed through parametrical FEAs. Accordingly, the number of rivets and the bearing ratio are the most influent parameters;
- Further studies are needed to completely assess the influence of geometrical and mechanical parameters on the fatigue performance of hot-driven riveted connections.

REFERENCES

- [1] A. Milone, M. D’Aniello, R. Landolfo, Influence of camming imperfections on the resistance of lap shear riveted connections. *Journal of Constructional Steel Research*, **203**, 107833, 2023.
- [2] M. D’Aniello, F. Portioli, L. Fiorino, R. Landolfo, Experimental Investigation on Shear Behaviour of Riveted Connections in Steel Structures, *Engineering Structures*, **32**(2), 516-531, 2011.
- [3] CEN. EN1993:1-9 - Eurocode 3 – Design of steel structures, Part 1-9: Fatigue, 2005, CEN, Brussel.
- [4] A. Milone, R. Landolfo, F. Berto, Methodologies for the fatigue assessment of corroded wire ropes: A state-of-the-art review. *Structures*, **37**, 787-794, 2022.
- [5] R. Tartaglia, A. Milone, M. D’Aniello, R. Landolfo, Retrofit of non-code conforming moment resisting beam-to-column joints: A case study. *Journal of Constructional Steel Research*, **189**, 107095, 2022.
- [6] A. Milone, R. Landolfo, A Simplified Approach for the Corrosion Fatigue Assessment of Steel Structures in Aggressive Environments. *Materials*, **15**(6), 2210, 2022.
- [7] R. Tartaglia, A. Milone, A. Prota, R. Landolfo, Seismic Retrofitting of Existing Industrial Steel Buildings: A Case-Study, *Materials*, **15**(9), 3276, 2022.
- [8] G. Di Lorenzo, R. Tartaglia, A. Prota, R. Landolfo, Design procedure for orthogonal steel exoskeleton structures for seismic strengthening. *Eng. Struct.* 275, 115252, 2023.
- [9] R. Tartaglia, M. D’Aniello, R. Landolfo, Seismic performance of Eurocode-compliant ductile steel MRFs, *Earthquake Engineering and Structural Dynamics*, 51(11), 2527-2552, 2022.
- [10] R. Tartaglia, M. D’Aniello, F. Wald, Behaviour of seismically damaged extended stiffened end-plate joints at elevated temperature. *Engineering Structures*, **24**, 113193, 2021.
- [11] R. Tartaglia, M. D’Aniello, R. Landolfo, Numerical simulations to predict the seismic performance of a 2-story steel moment-resisting frame, *Materials*. **13**(21), 1-17, 2020.
- [12] R. Tartaglia, M. D’Aniello, Influence of Transverse Beams On the Ultimate Behaviour of Seismic Resistant Partial Strength Beam-To-Column Joints. *Ingegneria sismica*, **37**(3), 50-65, 2020.
- [13] M. D’Aniello, R. Tartaglia, S. Costanzo, G. Campanella, R. Landolfo, A. De Martino, Experimental tests on extended stiffened end-plate joints within equal joints project. *Key Engineering Materials*, **763**, 406 – 413, 2018.
- [14] R. Tartaglia, M. D’Aniello, R. Landolfo, FREEDAM connections: advanced finite element modelling, *Ingegneria sismica*, **39**(2), 24-38, 2022.

-
- [15] R. Tartaglia, M. D'Aniello, R. Landolfo, G.A. Rassati, J. Swanson, Finite element analyses on seismic response of partial strength extended stiffened joints, *COMPDYN 2017* - 4952-4964, 2017. 10.7712/120117.5775.17542.
- [16] L. Fiorino, S. Shakeel, A. Campiche, R. Landolfo, In-plane seismic behaviour of lightweight steel drywall façades through quasi-static reversed cyclic tests, *Thin-Walled Structures*, **182**, 110157, 2023.
- [17] R. Landolfo, A. Campiche, O. Iuorio, L. Fiorino, Seismic performance evaluation of CFS strap-braced buildings through experimental tests, *Structures*, **33**, 3040-3054, 2021.
- [18] A. Campiche, S. Costanzo, Evolution of EC8 seismic design rules for X concentric bracings, *Symmetry*, **12**, 1-16, 2020.
- [19] L. Fiorino, A. Campiche, S. Shakeel, R. Landolfo, Seismic design rules for lightweight steel shear walls with steel sheet sheathing in the 2nd-generation Eurocodes, *Journal of Constructional Steel Research*, **187**, 106951, 2021.
- [20] A. Campiche, L. Fiorino, R. Landolfo, Numerical modelling of CFS two-storey sheathing-braced building under shaking-table excitations, *Journal of Constructional Steel Research*, **170**, 106110, 2020.
- [21] D. Cassiano, M. D'Aniello, C. Rebelo, Parametric finite element analyses on flush end-plate joints under column removal. *Journal of Constructional Steel Research*, **137**, 77–92, 2017. DOI: 10.1016/j.jcsr.2017.06.012
- [22] D. Cassiano, M. D'Aniello, C. Rebelo, Seismic behaviour of gravity load designed flush end-plate joints. *Steel and Composite Structures*, **26**(5), 621-634, 2018. DOI: <https://doi.org/10.12989/scs.2018.26.5.621>.
- [23] M. Bosco, M. D'Aniello, R. Landolfo, C. Pannitteri, P-P. Rossi, Overstrength and deformation capacity of steel members with cold-formed hollow cross-section. *Journal of Constructional Steel Research*, **191**, 107187, 2022. <https://doi.org/10.1016/j.jcsr.2022.107187>
- [24] A. Poursadrollah, M. D'Aniello, R. Landolfo, Experimental and numerical tests of cold-formed square and rectangular hollow columns. *Engineering Structures*, **273**, 115095, 2022. <https://doi.org/10.1016/j.engstruct.2022.115095>
- [25] A.F. Santos, A. Santiago, M. Latour, G. Rizzano, L. Simões da Silva, Response of friction joints under different velocity rates, *Journal of Constructional Steel Research*, **168**, 106004, 2020.
- [26] F. Berto, P. Lazzarin, Recent developments in brittle and quasi-brittle failure assessment of engineering materials by means of local approaches, *Materials Science and Engineering R: Reports*, **75**(1), 1-48, 2014.
- [27] P. Foti, M.R. Ayatollahi, F. Berto, Rapid strain energy density evaluation for V-notches under mode I loading conditions, *Engineering Failure Analysis*, **110**, 104361, 2020.
- [28] P. Foti, S.M.J. Razavi, M.R. Ayatollahi, L. Marsavina, F. Berto, On the application of the volume free strain energy density method to blunt V-notches under mixed mode condition, *Engineering Structures*, **230**, 111716, 2021.
- [29] Dassault. ABAQUS v. 6.14 User's Manual, Dassault Systemes.
- [30] J. Schijve, Fatigue of Structures and Materials – 2nd Edition, Springer, 2009.